Design and Optimization of a Reluctance-Torque-Assisted Synchronous Motor with High Efficiency and Low Torque Ripple

Qifang Lin, Shuangxia Niu, Weinong Fu
Email: eesxniu@polyu.edu.hk

Abstract — In this paper, numerical method coupled with a novel model is proposed and applied to permanent magnet synchronous motor with reluctance-torque-assisted, aiming to obtain a motor with high efficiency, low torque ripple and maintain a good saliency ratio. Time-stepping finite-element-method coupled with multi-objective genetic algorithm is used to perform the further optimization. Through the proposed design method, the efficiency of the motor under rated condition will be improved and higher than 92% which can satisfy IE4 standard and the torque ripple is no greater than 5%, which is relatively low compared with the initial design.

I. Introduction

Motors with reluctance-torque-assisted such as synchronous reluctance motor (SynRM) and the interior permanent-magnet motor (IPM) have high efficiency and wide range of operation speeds have been applied to lots fields like home appliances, industrial pumps, servo motors and electric vehicles [1]. SynRM is a single salient motor in which the rotor is constructed to employ the principle of reluctance torque to produce electromechanical energy conversion [2]. According to the topology of flux barrier, SynRM can be classified into two categories, namely, radial and transversely flux barriers. The structure of SynRM is relatively simple and the operation of SynRM is also straightforward. However, there are some demerits of SynRM. One of the demerits is the torque ripple of it is relatively large due to the discontinuous change of rotor magnetoresistance. In [2], rotor with radial flux barriers were investigated and the effects of the size of the flux barriers were studied in order to reduce the torque ripple and meanwhile maintain the saliency ratio. Another demerit of SynRM is the power density of it, which limits the application of SynRM to high power level occasions. In order to overcome these, PM-assisted SynRM (PMASRM) is proposed. Comparative study between SynRM and PMASRM was conducted in [3] and it was concluded that the PMASRM offers higher effective saliency and better output torque and power factor. Detail design parameters of radial flux barrier was studied in [4] and it was also found that the slot-pole combination with odd number of stator slots exhibits lower torque ripple compared with the one with even number. Moreover, radial PMs was tried in [4]. In [5] R-type and J-type flux barriers with transversely PMs was analyzed and C-shape flux barrier with transversely PMs was investigated in [6]. Recently, the length and width of flux barrier with radial PMs was studied in [7] and the length of airgap was also investigated. Besides SynRM and PMASRM, interior PM motors (IPM) was also widely used in electric vehicles and industrial applications for its low cost and flux weakening ability. In fact, IPM and PMASRM can both be classified as reluctance-torque assisted motor (RTAM). In [8], IPM motors with different arrangement of PMs, including I-shape, V-shape, U-shape, W-shape, as well as the surface mounted PM motors were analyzed and compared based on a general pattern. The cost of them was also taken into consideration.

In order to find the effects of flux barriers and PMs thoroughly, a novel model combined with numerical time-stepping finite element method is proposed and used to perform the selection process. Further, genetic algorithm is adopted to optimize the selected model in terms of the torque/PM volume, torque/current, torque ripple. And the saliency ratio of the optimized model will also be analyzed to estimate the flux weakening capability of it. The organization of the paper is as follows. In section II the novel numerical model and the design procedure will be illustrated firstly. In section III the effects of position of PMs, which is radially located or transversely located, and the thickness and width of it will be analyzed in terms of output torque, torque ripple. The optimal ratio between the width of stator teeth and the pole arc of rotor will be investigated. Different layers of flux barriers will be analyzed and compared in section IV, which is aiming to find cost effective design of RTAM.

II. Proposed Model and Optimization Procedure

The model for optimization is shown in Fig. 1. The material type of the rotor is changing automatically during the optimization process. “0” stands for vacuum and “1” is for PMs with specific excitation directions. For Material 1 to 3, if “1” is assigned, this means the material is PM with tangential direction away from air gap. For Material 4 to 6, “1” means the material is PM with tangential direction close to air gap. For Material 7 to 9, “1” stands for the PMs with radial direction point out center point and for Material 10 to 12 it means PMs point to center point. Material from 1 to 12 can be changed as PMs or vacuum according to the value assigned. A sequence will be generated to stand for the material combinations. For example, if the sequence is 000000111111, this stands for the exact topology shown in Fig. 1. At the specific condition, the model only has PMs with radial excited PMs and the rest materials are vacuum. With the proposed numerical model, topologies with different combinations of PMs can be generated automatically.

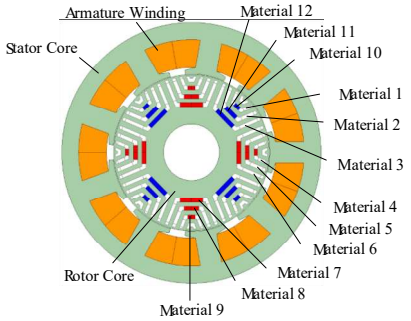

Fig. 1. Proposed FEM model for design of the PMA-SRM.

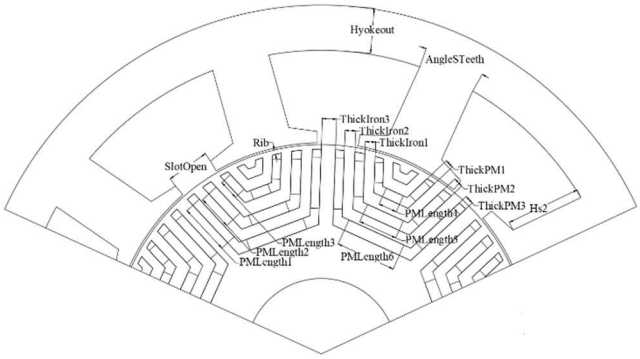

Fig. 2. Design parameters of the proposed model.

Not only the effects of material types to the performances of motor are investigated, but also the design parameters. The optimization of the design parameters is performed with multi-objective genetic algorithm after the material selection process. The detail design parameters of the proposed model are shown in Fig. 2. The optimization mainly focuses on the rotor part, including the thickness and length of PMs and the flux barriers. The crucial design parameters of the stator shown in Fig. 2 will be investigated.

The design procedure is as the flow chart described shown in Fig. 3. First, using the proposed model to generate topologies with different combination of PMs and the topologies can be selected according to their cogging torque and air gap flux density. Then, the one exhibits better performances will be selected out for further optimization. The optimized models of one-layer flux barrier RTAM, two-layer flux barrier RTAM and three-layer flux barrier RTAM will be analyzed and compared in terms of torque/current, torque/PM volume and saliency ratio.

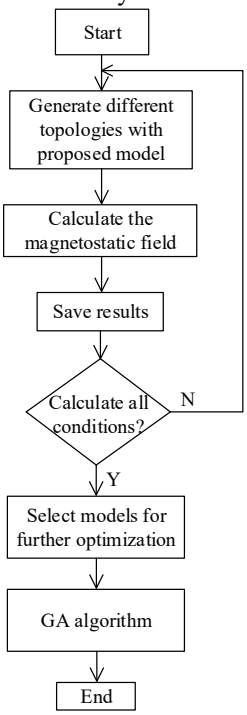

Fig. 3. The proposed design process.

The basic design parameters of the proposed model are shown in Table I. Motor with 9 stator slots and 8 rotor poles are selected and concentrated winding configuration is adopted. The rated speed of the motor is 3600rpm and the rated power is 11kW.

TABLE I
BASIC DESGIN PARAMETERS

Item	Parameters
Stator Slots	9
Rotor Poles	8
Stack Length	60 mm
Outer Diameter of Stator	185 mm
Current Density	3.6 A/mm^2
Silicon Steel	DW315_50
Rated Speed	3600 rpm
Rated Power	11 kW
PM Type	NdFe35
Airgap	0.5 mm

III. Effects of Design Parameters to Machine Performances

A. *Effects of Locations and Sizes of PMs*

The effects PMs, including their sizes and locations are analyzed in this part. The models used to perform the analyses are shown in Fig. 4. Fig. 4 (a) is motor with only radially located PMs and Fig. 4 (b) shows motor with only transversely located PMs.

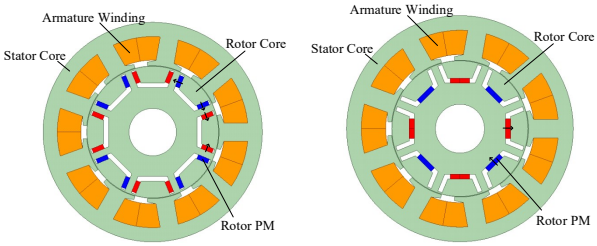

Fig. 4. Models used for analyses. (a)Model with radial PMs. (b) Model with transverse PMs.

The changing of output torque and torque ripple versus the thickness and length of radial PMs are shown in Fig. 5. And the sensitivity analysis of the thickness and length of radial PMs are shown in Fig. 6. The sensitivity of the parameter is defined as equation (1)

$$S(x_j) = \frac{x_{j0}}{O(x_0)} \cdot \frac{\partial O}{\partial x_j}\Big|_{x_i=x_0} = \frac{\Delta O/O(x_0)}{\Delta x_j/x_{j0}} \quad (1)$$

It can be found that the length of the radial PMs has obvious effect to the output torque of the motor than the thickness of it. And the sensitivity of the thickness of the PMs to the output torque is reducing as the thickness of PMs is increasing. This is caused by the saturation of the rotor core. The effect of length of radial PMs to the torque ripple is not obvious compared with it to the output torque. This means that the length of the radial PMs is helpful to generate output torque and contribute little to torque ripple. Thus, adding length of radial PM is a good option to increase the output torque.

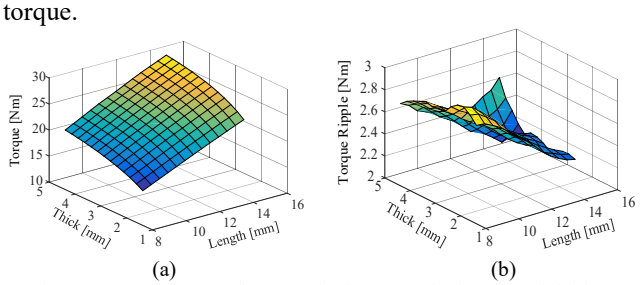

(a) (b)

Fig. 5. Output torque and torque ripple versus the length and thickness of raidal PMs. (a) Output torque. (b) Torque ripple.

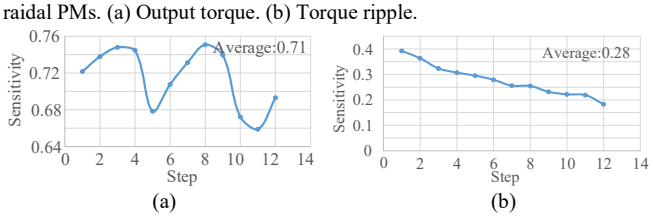

(a) (b)

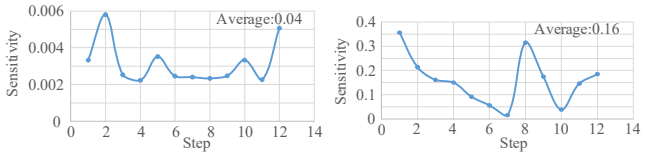

(c) (d)

Fig. 6. Sensitivity analyses of radial PM. (a) Sensitivity of the output torque versus length of PM. (b) Sensitivity of the output torque versus thickness of PM. (c) Sensitivity of the torque ripple versus length of PM. (d) Sensitivity of the torque ripple versus thickness of PM.

Fig. 7 shows the output torque and torque ripple versus the thickness and length of transverse PMs. It can be found that the increase of thickness of transverse PMs will increase the torque ripple significantly. The torque ripple can be suppressed as the length of transverse PMs is increased. Comparing the results shown in Fig. 5 and Fig. 7, it can be found that under the same volume of PMs, the radial PMs produce more torque compared with transverse PMs, which means the utilization of the radial PMs is higher than transverse PMs under this condition. Moreover, the torque ripple of the radial PMs is smaller than the transverse one. For sensitivity analysis, it can be found from Fig. 8 that the output torque is more sensitive to the length of PMs than it to the thickness of PMs. The torque ripple is more sensitive to the length of PMs than it to the thickness of PMs.

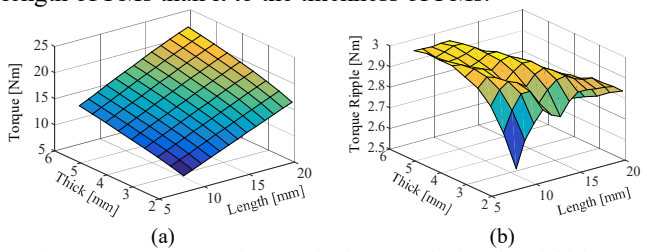

(a) (b)

Fig. 7. Output torque and torque ripple versus the length and thickness of transverse PMs. (a) Output torque. (b) Torque ripple.

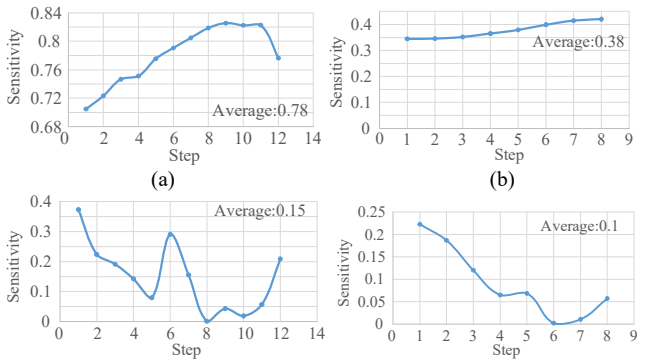

(a) (b)

(c) (d)

Fig. 8. Sensitivity analyses of transverse PM. (a) Sensitivity of the output torque versus length of PM. (b) Sensitivity of the output torque versus thickness of PM. (c) Sensitivity of the torque ripple versus length of PM. (d) Sensitivity of the torque ripple versus thickness of PM.

After the optimization of the two type motors in terms of the efficiency and torque ripple, the salient ratios of two optimized models under rated condition are analyzed. The saliency ratio is calculated according to equation (2)

$$\mathrm{SR} = \frac{L_d}{L_q} \tag{2}$$

Where L_d is the D-axis inductance and L_q is the Q-axis inductance. L_d and L_q are obtained through the Park transformation

$$\begin{bmatrix} L_d \\ L_q \end{bmatrix} = C^T * L_{abc} * C \tag{3}$$

Where C is the transformation matrix, L_{abc} is the matrix of self and mutual inductances. C is defined as

$$C = \sqrt{\frac{2}{3}} * \begin{bmatrix} cos\theta & sin\theta \\ cos(\theta - \frac{2*pi}{3}) & \sin(\theta - \frac{2*pi}{3}) \\ \cos(\theta + \frac{2*pi}{3}) & \sin(\theta + \frac{2*pi}{3}) \end{bmatrix} \tag{4}$$

The saliency ratio SR can be used to measure the flux weakening capability of the motor. The results are as Table II described. It can be found that the after optimization, PM utilization ratio of the radial PMs is higher than that of the transverse PMs. The saliency ratio of the transverse PMs one is higher than the one with radial PMs. The percentage of torque ripple of the motor with transverse PMs is higher than the one with radial PMs.

TABLE II
BASIC DESGIN PARAMETERS

Item	Value
Output torque of Motor with Radial PMs	26.82
Output torque of Motor with Transverse PMs	21.5
Torque ripple of Motor with Radial PMs	1.36
Torque ripple of Motor with Transverse PMs	1.35
PM Utilization Rate of Radial PMs	0.5
PM Utilization Rate of Transverse PMs	0.46
Saliency Ratio of Radial PMs	1.15
Saliency Ratio of Transverse PMs	1.31

B. Effects of the ratio between Stator Tooth Width and Rotor

The ratio between stator tooth width and the width of ThickIron3 described in Fig. 2 is investigated in this part. It is found that the ration between stator teeth width and ThickIron3 effect the salient ratio significantly. The effects of the ratio between stator tooth width and the rotor pole arc in terms of output torque and torque ripple are shown in Fig. 9. It is found that the better ratio between stator tooth width and rotor pole arc is around 0.61.

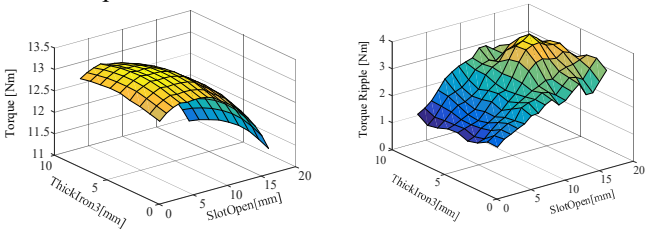

(a) (b)

Fig. 9. Output torque and torque ripple versus the length and thickness of transverse PMs. (a) Output torque. (b) Torque ripple.

IV. Comparison Between Different Layer Flux Barriers

Motors with different layers of flux barriers and different locations of PMs are analyzed and compared in this part. These models can be generated by the model shown in Fig. 1. For one-layer flux barrier motor, as shown in Fig. 11 (a), there are 16 different conditions. The initial results including the cogging torque and air gap flux density is shown in Fig. 11 (b). The models for further optimization for three motors shown in Fig. 11 (a), Fig. 12 (a) and Fig. 13 (a) are selected by criteria

$$OB_1 = B_{air}/B_{avg} * 0.6 - T_{cog}/T_{avg} * 0.4 \tag{3}$$

Where OB_1 is the objective value, B_{air} is the air gap flux density for specific models, B_{avg} is the average value of the air gap flux density for all models. T_{cog} is for the peak to peak value of the cogging torque.

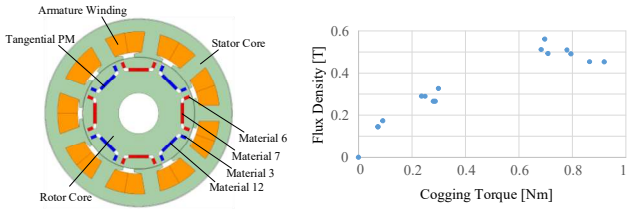

(a) (b)

Fig. 11. Output torque and torque ripple versus the length and thickness of transverse PMs. (a) Output torque. (b) Torque ripple.

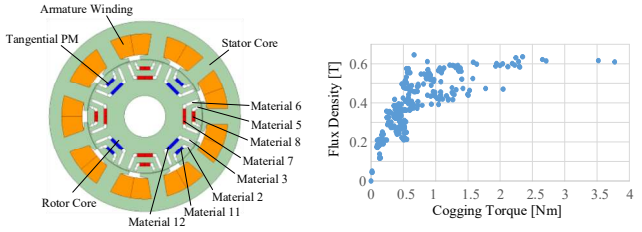

(a) (b)

Fig. 12. Output torque and torque ripple versus the length and thickness of transverse PMs. (a) Output torque. (b) Torque ripple.

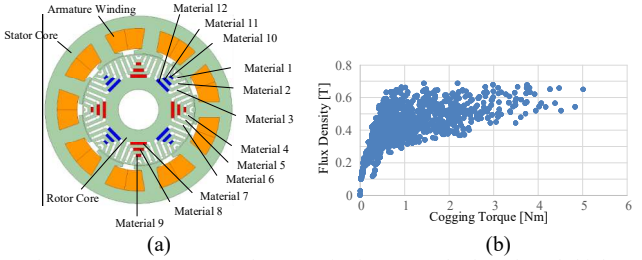

(a) (b)

Fig. 13. Output torque and torque ripple versus the length and thickness of transverse PMs. (a) Output torque. (b) Torque ripple.

The optimization results of three type motors in terms of PM utilization ratio, torque ripple and efficiency are shown in Table III. The former two motors meet the requirement output torque, torque ripple and the efficiency. The last one with three-layer doesn't exhibits such good performances compared with one-layer and two-layer motors. Within the given peripheral size, it can be found that the one-layer RTAM exhibits best performances in terms of PM utilization ratio,

TABLE IIITABLE III
PERFORMANCES OF THE THREE TYPES OF MOTORS AFTER OPTIMIZATION

Items	One-layer	Two-layer	Three-layer
Output Torque (Nm)	29.6	31.7	22.5
Peak-to-Peak Value of Total Torque (Nm)	1.91	1.51	3.20
Efficiency	94.5	94.1	82.3
Ld (mH)	15.1	14.7	15.3
Lq (mH)	11.8	11.3	10.1
Reluctance Torque (Nm)	3.9	3.6	4.4
Peak-to-Peak Value of Reluctance Torque (Nm)	1.06	1.98	3.2
Saliency Ratio	1.3	1.3	1.5
PM Utilization Ratio ($\times 10^3 kN/m^3$)	0.53	0.31	0.32

V. Conclusions

A novel FEM model is proposed in this paper to thoroughly investigate the performances of RTAM, including their output torque, torque ripple, efficiency, saliency ratio and how the design parameters of the motor effects its performances. It is found that the PM utilization ratio of the transverse PMs is higher than that of the radial PMs. The number of the layers of the flux barriers has little difference between the average value of the output reluctance torque of the motors with different layers of flux barriers is close under the same electric load, rotation speed silicon material.

VI. References

[1] Masayuki Sanada, Kenji Hiramoto, Shigeo Morimoto, Yoji Takeda, "Torque ripple improvement for synchronous reluctance motor using an asymmetric flux barrier arrangement," IEEE Trans. on Indus. Appl., Vol.40, No.4, pp.1076-1082, September, 2004.

[2] Takayoshi Matsuo, Thomas A. Lipo, "Rotor design optimization of synchronous reluctance machine", IEEE Trans. on Ener. Conv., June. 1994.

[3] Erich Schmidt, Wolfgang Brandl, "Comparative finite element analysis of synchronous reluctance machines with internal rotor flux barriers",in *Proc. IEMDC,* 2001, pp. 831-837.

[4] Peyman Niazi, Hamid A. Toliyat, Dal-Ho Cheong, and Jung-Chul Kim, "A low-cost and efficient permanent-magnet-assisted synchronous reluctance motor drive", IEEE Trans. on Indus. Appl., Vol.43, No.2, pp.542-550, March/April, 2007.

[5] Nicola Bianchi, Silverio Bolognani, Eiego Bon, Michele Dai Pre, "Rotor flux-barrier design for torque ripple reduction in synchronous reluctance and PM-assisted synchronous reluctance motors", IEEE Trans. on Indus. Appl., Vol.45, No.3, pp.921-928, May/June, 2009.

[6] Massimo Barcaro, Nicola Bianchi, Freddy Magnussen, "Permanent magnet optimization in permanent magnet assisted synchronous reluctance motor for a wide constant-power speed range", IEEE Trans. on Indus. Elec., Vol.59, No.6, pp.2495-2502, June, 2012.

[7] Pengyu Li, Wen Ding, Guoji Liu, "Sensitivity analysis and design of a high-performance permanent magnet assisted synchronous reluctance motor for EV application", IEEE Transportation electrification conference and Expo, June, 2018.

[8] Xiaoyu Liu, Qifang Lin, Weinong Fu, "Optimal Design of Permanent Magnet Arrangement in Synchronous Motors," Energies, 10(11), 2017, doi: 10.3390/en10111700.